



SURVEY BY AIRBORNE LASER SCANNER OF OPEN LARGE STRUCTURE: A CASE STUDY OF POMPEII AMPHITHEATRE

Massimiliano Pepe

Department of Sciences and Technologies (DIST), University of Naples "Parthenope", Italy

E-Mail: massimiliano.pepe@uniparthenope.it

ABSTRACT

The purpose of this paper is to show the potential of Airborne Laser Scanner (ALS) in the survey of large and open structures in the Cultural Heritage field. Nowadays, this technology is becoming spread in the field of Cultural Heritage thanks to the possibility to obtain a large number of points in a short time. In fact, the latest generation of ALS sensors are able to acquire up to several million measurements per second and to generate an elevated point density. In addition, if this sensor is combined with digital camera, it is possible to obtain even RGB colour information. In this paper are described the features, methods and techniques for acquisition by ALS system. In particular, it is presented a wide analyse of the three dataset (calibration, laser distance measurements and Position-Orientation System data). The assembly of these datasets allows obtaining the correct georeferencing of the point clouds. A case study of a survey carried out by ALS system on the archaeological site of Pompeii (Italy) is presented. In this case, all the steps necessary to realize the survey are described (planning, acquisition and post-processing task). Also, starting from the point clouds, in CAD environment a classic representation (in a suitable scale) of Roman amphitheatre is showed.

Keywords: ALS, aerial survey, cultural heritage, flight planning, direct georeferencing, ALS calibration, LiDAR.

INTRODUCTION

Airborne Laser Scanning (ALS) is an active Remote Sensing technique based on Light Detection and Ranging (LiDAR) measurements from an airborne or helicopter [1;2] and most recently, even from Unmanned Aerial System (UAS). While fixed-winged aircraft are typically used for the acquisition of large project areas, rotary wing are preferred for linear feature (e.g. for corridor mapping) or for difficult topography where it is required a high density of points [3]. The advantage of ALS sensor than optical sensors is less dependent on the weather, season and time of the day in data collection. In addition, it can generate 3D topographic surface information more rapidly [4; 5].

ALS sensors providing the range measurements between the laser scanner and the Earth topography (terrain, building, power line, etc.) by the time-of-flight between the emitted and backscattered laser pulse. Also, the airborne LiDAR sensor produces a georeferencing point clouds. In addition to the coordinate information is normally available too, the intensity and return echoes for each pulse sent to the target. Indeed, recent ALS sensors can store several multiple reflections and register the full shapes of the returning echoes [6]. So, a first echo (*first pulse*) and a number of successive echoes, until the last (*last pulse*), can be used in order to recognize some features of the measured target.

The precise position and orientation of the sensor is obtained from the integration between Global Navigation Satellite Systems (GNSS) and Inertial Systems (INS) (GNSS/INS).

In order to calculate with high precision the Position and Orientation (POS) of ALS sensor, it is necessary to perform a calibration task. In this way, it is possible to know, instant by instant (generally, at the

frequency of 1Hz), the positioning position and attitude of ALS sensor.

Summarizing, the correct georeferencing of point clouds data from ALS sensors can be obtained with the help of the three data sets: calibration data and mounting parameters, laser distance measurements with their respective scanning angles and position and Orientation system data [7].

Application of ALS data in Cultural Heritage and 3D building environment

ALS data are currently used in a wide range of scientific applications especially in environmental issues [8, 9]. However, in the last years, the survey with ALS is spreading even in Cultural Heritage (CH) environment.

The use of ALS data in this context, it was mainly addressed to the survey of interesting landscape, as shown in the paper reported in the book "*Heritage Management of Farmed and Forested Landscapes*" [10]. A comprehensive description of the different investigations in archaeology obtained with the LiDAR sensor is shown in the paper of Campana et al. [11] and in the paper of Bewley et al. [12]. In this latter paper an ALS survey of famous Stonehenge World Heritage Site is described where the analysis of ALS data and the integration with other sensors, it involves to detection of unknown sites. Other experience of the survey in CH environment where Terrestrial and Aerial Laser Scanning data are fully integrated, are reported in several works of literature [13; 14; 15].

However, in urban and architecture fields, the applications by ALS data are numerous. Indeed, many building modelling algorithms have been developed in order to extract shape and size of the buildings [16; 17]. Also, while the development of LiDAR technique in the



urban environment is common since several years, the applications in archaeology and Cultural Heritage fields are still object of experimentation. This is mainly due to the complexity of these structures. In fact, they require a high density and accuracy of the point clouds that only recently ALS systems are able to achieve.

Organization of the article

In order to explain the potentiality of the ALS sensors in CH applications, the paper is divided in two parts.

In first part of the paper, the essential features, methods and processes data of each dataset that led the direct georeferencing of point clouds are discussed.

In the second part of the paper, a case study of the application of the LiDAR sensor in CH environment is showed.

GEOREFERENCING AIRBORNE LiDAR DATA

Laser distance measurements and point density

ALS sensors produce a dense point cloud of the object: greater it is the density, greater is the level of the detail of the object under investigation. The parameters that determine the point density of point cloud and, consequently the ALS flight planning, are diverse [6;18].

The first parameter that affects the points density is the *scanning frequency* that is the number of pulses or beams emitted by the laser instrument in 1 second. The ALS sensors have different scanning mechanisms (oscillating, sinusoidal, fiber scanner, rotating polygon, etc.). Each scanning mechanisms produces a different spatial distribution of the points. The most widespread configurations of the spatial distribution points (figure 1) and the relative model developed by several manufacturers are reported below [18]:

- seesaw pattern (sawtooth), used by Optech company in the model ALTM 3100.
- seesaw pattern stabilized equivalent (sinusoidal), used by Leica Geosystems in the ALS50 e ALS60.
- parallel line pattern, used by Riegl company for the model LMS-Q680;
- elliptical pattern, used by TopEye AB company for the model TopEye Mk II.

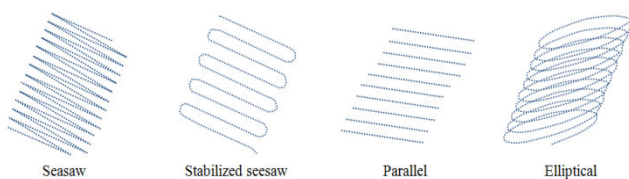


Figure-1. Several spatial distribution points [6].

In seesaw and stabilized seesaw pattern, the pulse is directed across the scanning swath by an oscillating mirror, and returns are continuously generated in both directions of the scan. Although this configuration is

designed to preserve the spacing between returns, in practice, pulse density is not uniform [6]. In the parallel line pattern, a rotating polygonal mirror directs pulses along parallel lines across the swath, and data are generated in one direction of the scan only. The elliptical pattern is obtained via a rotating mirror that revolves about an axis perpendicular to the rotation plane. Recent development in laser scanner technology led to realizing of a system that provides three scan patterns (seesaw, stabilized seesaw and parallel), all in a plane nominally orthogonal to the longitudinal axis of the scanner, nominally centered about nadir [19]. Of course, for each scanning mechanisms corresponds a specific formula for the calculation of the density of points. A work that describes the essential formula for ALS sensor is the paper of Batislava [20].

Another parameter that influences the point density is the *beam divergence*. It refers to the increase in beam diameter that occurs as the distance between the laser instrument and a plane that intersects the beam axis increases. Typical beam divergence settings range from 0.1 to 1.0 millirad. This parameter is very important in the ALS survey because it determines the penetration level of the pulse in forests and other vegetated areas, the level of detectable detail, the sharpness with which outlines of buildings and other objects can be recorded, and the level of eye safety [21].

The *Scanning angle* is the angle the beam axis is directed away from the “*focal*” plane of the LiDAR instrument: greater is the its value, lower is the point density. Sometimes, in a similar way to the photogrammetric terminology, this angle is called FOV (Field Of View).

In order to increase the density point in the construction of the flight planning, it is necessary changes one or more parameters above mentioned. In addition, there are other two ways for increase point density. In the first case, it is possible increase the density point by the building of a suitable flight planning designed with strips crossed at 90°. This approach is widespread especially in survey on dense urban area or in zone of particular interest where it has requested further details of spatial objects. A second way regarding a special LiDAR technology. Indeed, in last year has been developed a special technology called Multiple Pulses in Air Technology or MPiA which allows using at higher pulse rates than previously possible [22]. By allowing the airborne ALS system to fire a second laser pulse prior to receipt of the previous pulse’s reflection, the pulse rate at any given flying height can be effectively doubled. Beyond to the system (MPiA) by Leica Geosystems, other company have developed a special technology that allow increase the density point, as “*continuous multipulse*” (CMP) by Optech and “*multiple time around*” (MTA) by RIEGL. Irrespective of these differences in the name, their common adoption of this special technique means that the laser rangefinder can fire a new pulse towards the ground without having to wait for the arrival of the reflection of the previous pulse at the instrument.



Positioning and orientation data

The POS of the ALS system allows knowing every moment the position and the attitude of the sensor thanks the integration of GNSS and INS systems. The benefits of a GNSS/INS integration are that the INS estimates can be corrected by the GNSS data and that the INS can provide position and angle updates at a quicker rate than GNSS. In addition, GNSS signal losses or change of GNSS constellations may occur and the INS can continue to calculate position, velocity and orientation angles during outages [23; 24]. Depending on the architecture of integration, the integration may present different cases: loosely coupled, tightly coupled integration and tightly coupled [25].

In general, the post processing analysis of the trajectory is realized by standard methodology, known as Differential GPS (DGPS) DGPS is used to eliminate typical errors in this positioning environment, such as errors in the receiver and the Satellites clock, multipath effect, ionosphere and troposphere delay. By using single or multiple base stations set up over known surveyed locations, to collect satellite data at the same time as the mobile GNSS receiver, very accurate positioning of the mobile receiver can be achieved [26].

In order to verify the estimated accuracy, potential anomalies, data gaps and systematic errors occurred during the flight mission, the diverse software that manage the trajectory of the aircraft allow a quality check. Indeed, by the use of suitable plots (estimated horizontal and vertical accuracy, PDOP, etc.) it is possible to analyse the quality of GNSS/INS data.

Calibration data

The calibration process has the purpose to know the spatial configuration of the several elements of the ALS sensors and in general, it consists of three calibration types [27]:

- laboratory;
- platform;
- in-flight calibration.

The aim of the laboratory calibration is the setting of the individual system components. In this task, the eccentricity (also called lever arm) and misalignment between the laser mirror and the IMU as well as the eccentricity between the IMU and the sensor reference point are determined. Generally, this task has performed by LiDAR manufacturer in order to obtain high accuracy in the measure of this eccentricity.

In the platform calibration, the eccentricity between the sensor reference point, the IMU and the GNSS antenna is determined. Lever arm calibration can be done using different approaches; quite common and easy methods consist in measuring the lever arms using land-survey techniques. The reference axis of the several elements of LiDAR system is sketched in Figure-2.



Figure-2. Aircraft body coordinate system (left) and reference axes of the laser and IMU in bottom view (right).

The in-flight calibration step allows refining the characteristic parameters and to determinate biases of the system measurements. In this task, take a particular importance the determination of the angular misalignment between the laser head and the IMU [28]. In general, there is not a standard procedure to calculate this angles misalignment. A method of investigation consists in to analyse the errors (roll, pitch and heading errors) that individual these angles involve in the correct georeferencing of point clouds. The first step for investigation of these misalignment angles involves in the build a suitable flight planning. Because all LiDAR measurement are based on the trajectory, a good acquisition of the ALS data during the flight mission is essential for calibration data. This mean acquiring the data with the following recommendations [29]:

- no turbulent flight condition;
- the distance between the ground reference GNSS base stations and the GNSS receiver(s) on-board the flying carrying platform is suggested 30 km to 50 km in a flat and obstacle-free area.
- position (3D) dilution of precision (PDOP) value lower to 3;
- roll angle contained in 10° .

In general, ALS manufacturers have implemented specific procedures in order to calculate the misalignment angles. Therefore, every calibration sensor involves in a different pipeline and the use of diverse package software. At the end of acquisition data and the calibration processing, it is necessary to perform a task for bore sight check. Indeed, if the calibration is not successful, the position of the points will be wrong. If there is a roll error, the point clouds move the data up on one side of the swatch and down on the other side of the swatch while if the pitch angle was not calculated correctly, error moves all the data forward or backward. The error in determining the heading misalignment led a wrong georeferencing of point clouds except in the data at nadir, shifting and deforming the object [30]. This check task can be obtained loading in a software able to manage LiDAR data two opposing flight line (FL) at high altitude. In this way it is possible to verify the roll and the pitch error. Loading two parallel FL (preferably at high altitude) it is possible to check the heading error. In the latter case, loading two



crossing high altitude FL, it is possible check both the heading and the torsion error. The torsion error is due to changing of speed and acceleration between the mirror and the angular encoder and if this effect is not corrected, it causes a small, but systematic misreading of the angle, which is manifested by the ends of the scan rising too high or dropping too low [31].

Direct georeferencing

The direct georeferencing equation allows obtaining, in a specific mapping frame, the spatial coordinates of the point clouds by the assembly of the three datasets described previously [32]:

$$\bar{r}_{ground} = \bar{r}_{GNSS} + R_w \cdot R_G \cdot R_{ins} \cdot (\bar{r}_{ecc} + R_m \cdot R_s \cdot \bar{\rho}) + \bar{r}_{re}(1)$$

\bar{r}_{ground}	vector of observed ground coordinates;
\bar{r}_{GNSS}	vector of observed absolute position on the aircraft platform at the GNSS receiver;
R_w	rotation matrix from the WGS-84 datum to a local ellipsoidal reference frame;
R_G	rotation matrix from the local gravity frame to the ellipsoidal frame by the Deflection of the Vertical (DOV).
R_{ins}	rotation matrix from the body frame to the local level frame;
\bar{r}_{ecc}	vector of offsets between the laser transmission point and the phase centre of the GNSS antenna in the body frame;
R_m	rotation matrix containing the boresight angular values which rotate between the body frame and laser scanning frame;
R_s	rotation by a value equal to the observed scan angle;
$\bar{\rho}$	observed range observation $[0, 0, -\rho]^t$;
\bar{r}_{re}	vector of random error components of the observation in the same reference frame as the laser point.

The values ξ, η of DOV (the two mutually-perpendicular components of the deflection of the vertical vector in the north and east directions, respectively) to put in the matrix R_G depend on the position and altitude of the aerial survey. Also, the choose of the type of the models (geopotential or local) in order to obtain the values of the deflection of vertical must be defined by several simulations [33].

CASE STUDY

Brief history of the site under investigation

The survey concerns the archaeological site of Pompeii (Italy) and in particular the famous Roman amphitheatre (Figure-3).



Figure-3. Area study: archaeological site of Pompeii. (Image taken from Google Earth).

This structure, located in a marginal area of the archaeological site, could hold up to 20,000 spectators [34]. The amphitheatre of Pompeii is the oldest surviving Roman amphitheatre built around 70 BC [35]. The shape of the amphitheatre is elliptical where the major and minor semi-axes have a length of about 68 meters and a width of 52 meters; the height of this structure is about 13 meter.

Outline of the survey

In order to describe all the operations required for the survey of the *Roman amphitheatre* by ASL system, it is necessary divide this task in the following several steps:

- Description of ALS sensor used for this purpose;
- Calibration of the sensor;
- Flight planning and data acquisition;
- Post-processing ALS data;
- Representation of the structure.

ALS Sensor

The LiDAR mission has been performed with Leica Geosystems ALS50 II sensor. This system emits laser radiation with wavelength of 1064 nm and could be operated at maximum of 6000m. Maximum PRF goes up to 200 kHz and scan rate to 90 Hz in 0.1 Hz increments via the graphical user interface. System FOV is adjustable over the range of 0-75 degrees, in 1-degree increments. The maximum value of FOV is related at the characteristics of the aircraft. The ALS 50 II system provides a sinusoidal scan pattern in a plane nominally orthogonal to the longitudinal axis of the scanner, nominally centered about nadir [36].

Platform calibration and in-flight calibration

The first tasks for platform calibration consist in the calculation of the lever arms on the aircraft. In this case, the survey of the calibration and acquisition data has been carried out using a Partenavia P68 aircraft. The coordinate of the several elements (GNSS antenna, IMU, LiDAR) has been obtained by Pentax R-325(N) total station. By routine developed in Matlab software, it has possible to calculate the lever arms (Table-1).

**Table-1.** Lever arms values (in platform calibration).

	X(m)	Y(m)	Z(m)
Reference point of the LiDAR sensor	0	0	0
GNSS antenna	0.045	0.192	-1.179
IMU	0.232	0.081	0.045

Subsequently, it is possible to proceed to the next phase, that is the in-flight calibration. In order to simplify the description of the different operations, this task can be divided into the following steps:

- Build a suitable mission planning;
- Acquisition of airborne data;
- Terrestrial survey;
- Post-processing of terrestrial and airborne data.

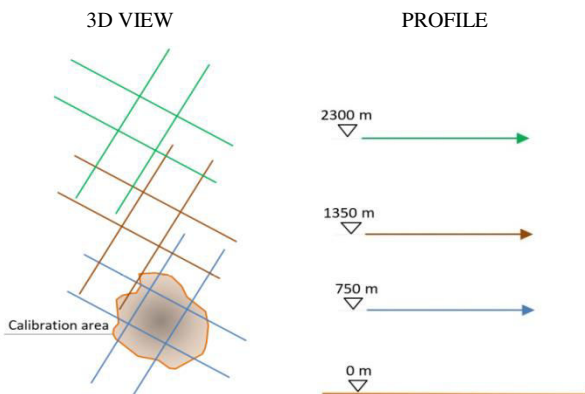
The flight planning calibration has been performed with Leica Geosystems software for ALS system on

specific area [37]. The elevation terrain model used in the software has been the SRTM (Shuttle Radar Topographic Mission) [38, 39]. The use of this DEM has allowed complying the density points designed in the flight planning. In this case, the ground is fairly flat. However, if the survey area shows somewhat accentuated soil morphology, it is preferable to use a more accurate and detailed DEM. The flight planning, build for the characteristic of P68 aircraft (twine engine and high fixed wing) whose acquisition speed is 120 kts (about 222 km/h), consists of ten strips: three strips at low altitude (700 m), three strips at middle altitude (1350 m), four FL at high altitude (2300 m). The three altitude considered are the so-called “*relative height*”, that is the elevation the aircraft than the terrain. Therefore, beyond of the name of the FL and the AMSL, acronym the Above Mean Sea Level (also known as “*absolute height*”) the ALS parameters used in the flight planning are indicated in the Table-2.

Table-2. FL parameters in the flight planning calibration.

Line (#)	Direction (°)	AMSL (ft)	FOV (°)	PR (Hz)	MPIA	Laser Current %
A13	163	2345	45	110	SPIA	20
A14	253	2345	45	110	SPIA	20
A14	163	2345	45	97	SPIA	19
A15	163	4478	45	150	MPIA	49
A16	253	4478	45	150	MPIA	49
A16	163	4478	45	97	MPIA	37
A17	163	7595	45	100	MPIA	90
A18	253	7595	45	100	MPIA	90
A19	163	7595	45	100	MPIA	90
A17	253 switch	7595	45	100	MPIA	90
A18	163	7595	45	97	MPIA	88

A graphical representation of the flight planning realized, is shown in Figure-4.

**Figure-4.** Sketched of calibration flight planning.

Subsequently, a terrestrial survey with acquisition of 10 GCPs (Ground Control Points) has been performed. Using DGPS technique, the coordinates of this point have been elaborated by LGO software. The maximum horizontal and vertical errors on the GCPs are respectively 5mm and 9mm.

By adopting the procedure and using the supplied software of the sensor manufacturer, it has possible obtain all the parameters to be defined in the calibration process. Lastly, a LiDAR software has been used in order to compute the elevation difference between surfaces from individual strips and a mean surface and the its average value. The values obtained by this approach are on the order of a few centimetres.



Mission planning on the area study

In this case study, the area of interesting (archaeological site) has been extrapolated from the calibration flight. However, to achieve the same point density, an example of flight planning parameters realized by Leica software is shown below (Figure-5). In particular, the software calculates all the flight planning parameters, in order to obtain an average point density of 15pts/m² considering an acquisition speed of 90 kt.

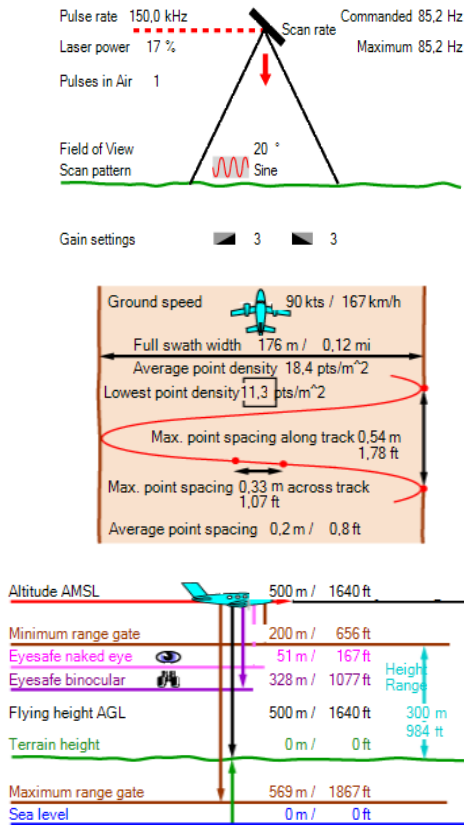


Figure-5. Example of flight planning parameters on the area study using Leica AeroPlan80 Standalone.

In general, from the experience of the author, it is recommendable an increase of the 15% than the designed average density point to take account of any issues, such as the uncertainty in the terrain model adopted and/or the environmental conditions.

Indeed, in relation to environment condition, especially the wind can be influence the compliance of the flight planning. Indeed, if the wind is present in the same direction of the direction of fly, the aircraft increase its speed and this led a reduction of the point density. As reported in the following diagram (Figure-6), it is possible to note the trend of average density point varying the speed of the aircraft.

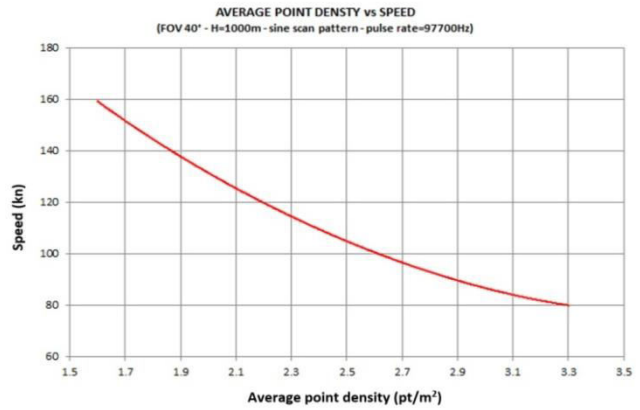


Figure-6. Variation of the average density points respect to the acquisition speed.

Analysis of POS data

Initial processing of POS data has been realized by Waypoint GrafNav software. In the flight mission, the maximum distance from the base station (used to perform DGPS) and the area survey has been of about 15km. This base station (Figure-7) belongs to the network of permanent stations (CORS) established by the local public administration (Campania Region).

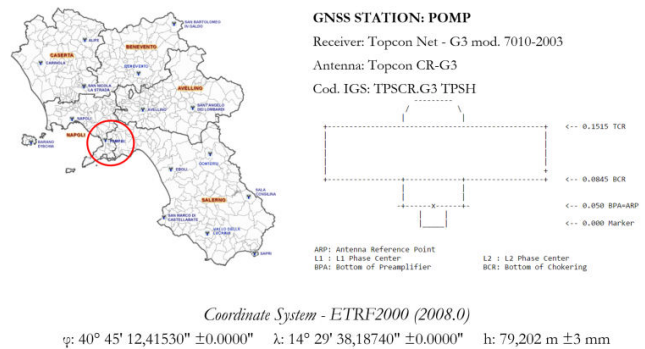


Figure-7. GNSS base station.

The use of the Leica Geosystems IPAS Pro software for the management of GNSS/IMU data and then by Leica Geosystems ALS Post Processor software have allowed the generation of point clouds in LAS format (LASer File Format Exchange Activities).

LAS format is a public file for the interchange of 3-dimensional point cloud data between data users maintaining information specific to the LiDAR nature of the data. Indeed, due its capability to hold tens to hundreds of millions point, it has become a standard for storing and distributing the acquired points [40].

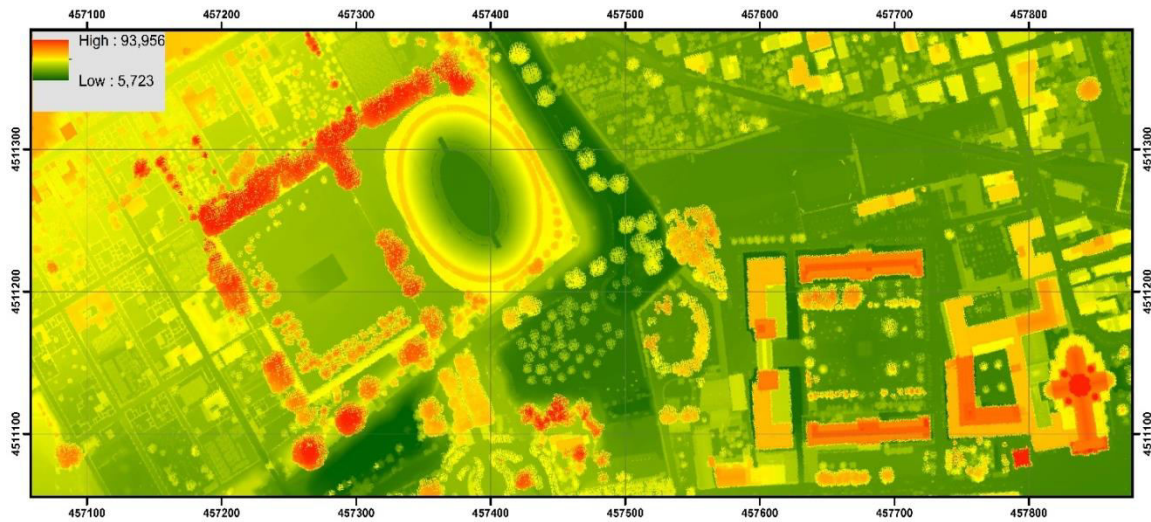


Figure-8. Map of elevation.

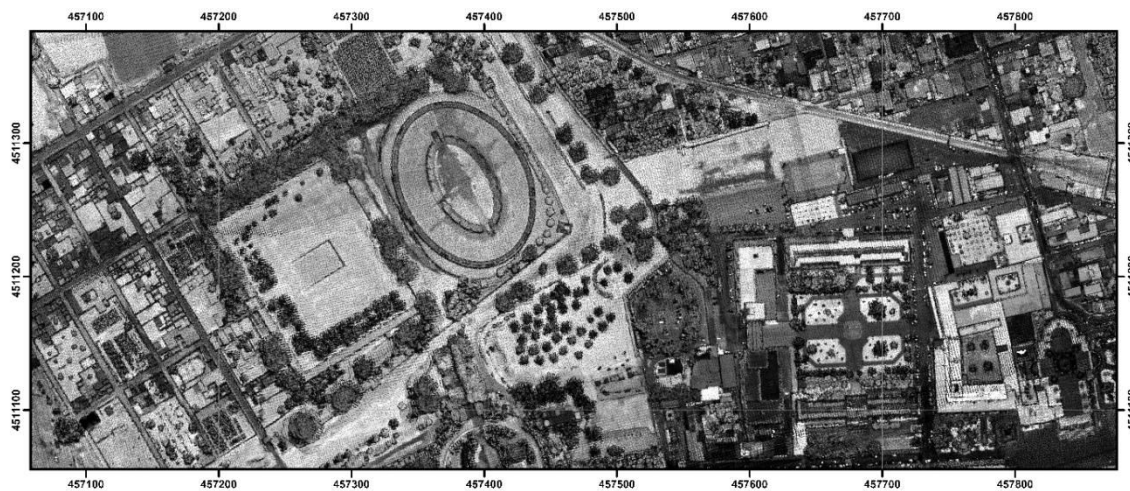


Figure-9. Map of intensity (values from 0 and 255 - 0 black, 255 white).

Map projection for three-dimensional point cloud

The point clouds have been generated in geographic coordinate. For this reason, the projection in a coordinate plane system has been performed. Recently the Italian government, acknowledging the indication reported in the European Directive INSPIRE (Technical Guidelines Annex I - D2.8.I.1) has adopted a new reference system called ETRF2000 (2008.0). Also, the reference system used for the survey is the RDN2008/TM33. In addition, the coordinate in elevation of the point clouds have the ellipsoidal height (h). Therefore, because in the survey is required the orhometric height (H), knowing the geoid undulation model (N), it has possible obtain this height by suitable algorithm [41]. By transforming the point clouds in raster using feature values contained in the LiDAR information, it is possible to obtain the following several

representations: elevation model (Figure-8) and intensity map (Figure-9).

From point clouds to representation

The intensity and elevation maps have allowed to draw the contours and the characteristic elements of the structure.

Because in some parts of the Roman amphitheatre there was low vegetation, thanks to use of the intensity map, it has been to discern the area within in the structure with and without vegetation.

In addition, from the point clouds, it has possible to extrapolate the elevation coordinate of the drawn object. A traditional representation derived from Computer-Aided Drafting (CAD) environment (plan and profile), is shown in the Figure-10.

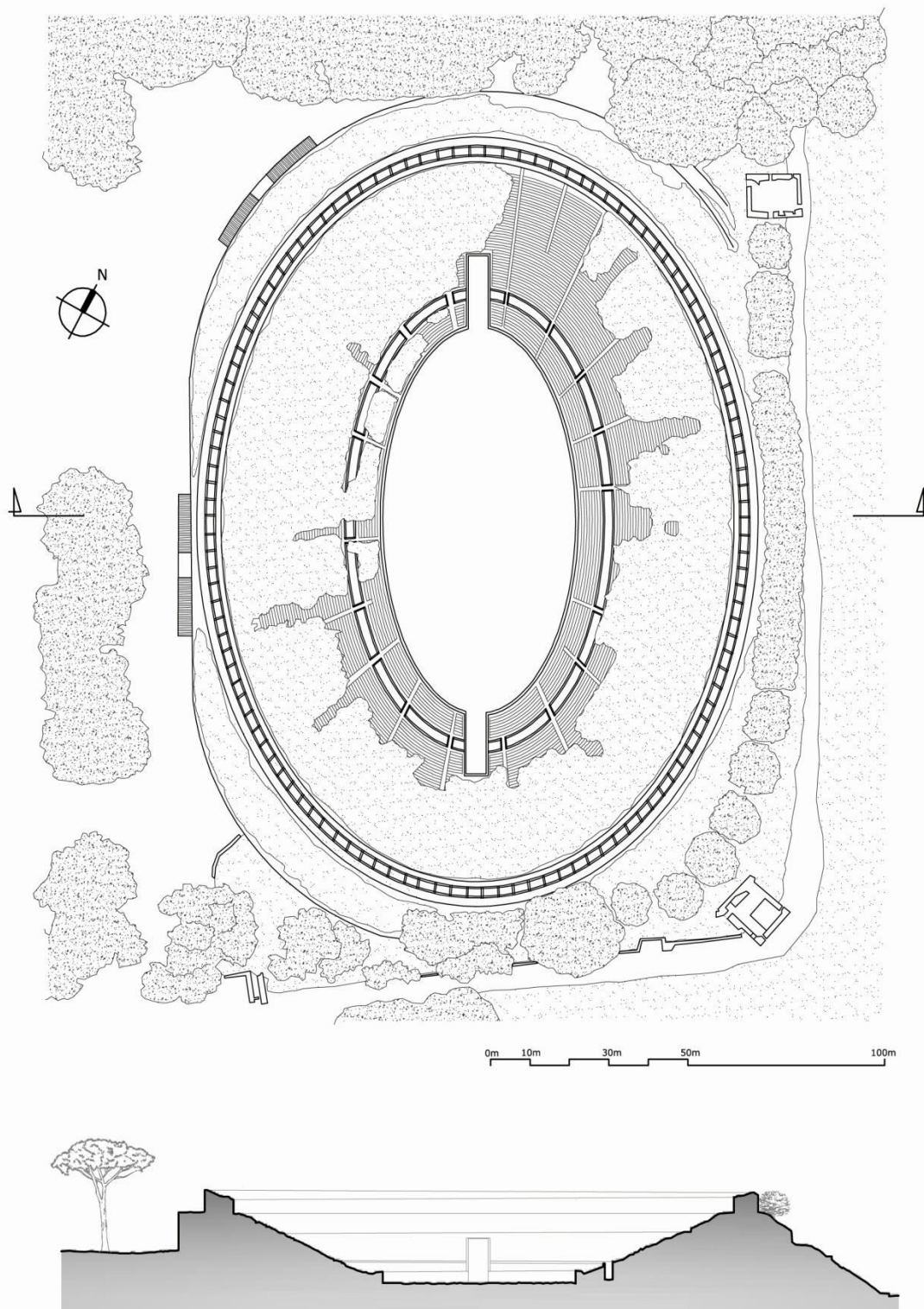


Figure-10. Plan and profile of the Pompeii's amphitheatre derived by ALS data.

CONCLUSIONS

The survey obtained by ALS data has enabled obtain in short times a dense point clouds very useful for the representation of the ancient artefact, as shown in the case study.

Also, the survey with ALS sensor represents a valuable tool for the detection of wide open structures in Cultural Heritage environment.

However, taking into account the accuracy of the several steps which led to the generation of the point cloud and the point density, the author claim a suitable scale of



representation is 1:500. In addition, the vertical parts of the structure investigated needs of integration because the ALS sensor has not been able to generate point on the side of the structure. This task can be obtained both the Terrestrial Laser Scanner and/or Close Range Photogrammetry survey. Indeed, always more often the integration of more survey techniques is adopted in complex study areas.

Despite the point density has not allowed a refined representation of some details, considering the huge technological development of this sensor and the ability to obtain dense point clouds, the ALS sensors will be able to overcome these limitations and then it can be used in order to represent objects with greater detail.

ACKNOWLEDGEMENTS

The author thanks Avioriprese srl, aerial survey company, for providing the airborne and the cooperation in the flight mission.

REFERENCES

- [1] Beraldin J.A.; Blais F.; Lohr U. 2010. Laser scanning technology. In: Vosselman, G., Maas, H.-G. (Eds.), *Airborne and Terrestrial Laser Scanning*. Whittles Publishing, Dunbeath, Scotland, UK. pp. 1-42.
- [2] Schaer P.; Skaloud J. & Tomé P. 2008. Towards in-flight quality assessment of airborne laser scanning. In XXI ISPRS Congress (No. TOPO-CONF-2009-001).
- [3] Pfeifer N. & Briese C. 2007. Geometrical aspects of airborne laser scanning and terrestrial laser scanning. *International Archives of Photogrammetry, Remote Sensing and Spatial Information Sciences*. 36(3/W52): 311-319.
- [4] Ackermann F. 1999. Airborne Laser Scanning-Present Status and Future Expectations, *ISPRS Journal of Photogrammetry and Remote Sensing*. 54(2-3): 64-67.
- [5] Shan J. & Aparajithan S. 2005. Urban DEM generation from raw LIDAR data. *Photogrammetric Engineering & Remote Sensing*. 71(2): 217-226.
- [6] Matikainen L.; Lehtomäki M.; Ahokas E.; Hyyppä J.; Karjalainen M.; Jaakkola A.; Kukko A.; Heinonen T. 2016. Remote sensing methods for power line corridor surveys, in *ISPRS Journal of Photogrammetry and Remote Sensing*. 119: 10-31, ISSN 0924-2716.
- [7] Wehr A. & Lohr U. 1999. Airborne laser scanning-an introduction and overview. *ISPRS Journal of photogrammetry and remote sensing*. 54(2): 68-82.
- [8] Lefsky M. A., Cohen W. B., Parker G. G. & Harding D. J. 2002. LIDAR remote sensing for ecosystem studies: LIDAR, an emerging remote sensing technology that directly measures the three-dimensional distribution of plant canopies, can accurately estimate vegetation structural attributes and should be of particular interest to forest, landscape, and global ecologists. *BioScience*. 52(1): 19-30.
- [9] Zhang K., Chen S. C., Whitman D., Shyu M. L., Yan J. and Zhang C. 2003. A progressive morphological filter for removing nonground measurements from airborne LIDAR data. *IEEE transactions on geoscience and remote sensing*. 41(4): 872-882.
- [10] Byrnes E. 2010. Heritage Management of Farmed and Forested Landscapes in Europe.
- [11] Campana S., Sordini M., Bianchi G., Fichera G. A. & Lai L. 2012. 3D recording and total archaeology: From landscapes to historical buildings. *International Journal of Heritage in the Digital Era*. 1(3): 443-460.
- [12] Bewley R. H., Crutchley S. P. & Shell C. A. 2005. New light on an ancient landscape: LIDAR survey in the Stonehenge World Heritage Site. *Antiquity*. 79(305): 636-647.
- [13] Fryskowska A., Walczykowski P., Delis P. & Wojtkowska M. 2015. ALS and TLS data fusion in cultural heritage documentation and modeling. *The International Archives of Photogrammetry, Remote Sensing and Spatial Information Sciences*. 40(5): 147.
- [14] Kedzierski M. and Fryskowska A. 2014. Terrestrial and Aerial Laser Scanning Data Integration Using Wavelet Analysis for the Purpose of 3D Building Modeling. *Sensors*: 12070-12092.
- [15] Julge K. & Ellmann A. 2014. Combining airborne and terrestrial laser scanning technologies for measuring complex structures. In *Environmental Engineering. Proceedings of the International Conference on Environmental Engineering*. ICEE (Vol. 9, p. 1). Vilnius Gediminas Technical University, Department of Construction Economics & Property.
- [16] Elaksher A. F. & Bethel J. S. 2002. Reconstructing 3d buildings from LIDAR data. *International Archives of Photogrammetry Remote Sensing and Spatial Information Sciences*. 34(3/A): 102-107.
- [17] Zhou Q. Y. & Neumann U. 2008. Fast and extensible building modeling from airborne LIDAR data.



- In: Proceedings of the 16th ACM SIGSPATIAL international conference on Advances in geographic information systems. ACM.
- [18] Triglav Č., M., Crosilla F. and Kosmatin F. M. 2010. Theoretical LIDAR point density for topographic mapping in the largest scales. *Geodetski vestnik*. 54(3): 403-416.
- [19] Gatzliolis D., Andersen H. E. 2008. A guide to LIDAR data acquisition and processing for the forests of the Pacific Northwest. US Department of Agriculture, Forest Service, Pacific Northwest Research Station.
- [20] Baltsavias E. P. 1999. A comparison between photogrammetry and laser scanning. *ISPRS Journal of photogrammetry and Remote Sensing*. 54(2): 83-94.
- [21] Lemmens M. 2011. *Geo-information: technologies, applications and the environment* (Vol. 5). Springer Science & Business Media. pp. 158-160.
- [22] Petrie G. 2011. Airborne topographic laser scanners. *GEO Informatics*. 14, pp. 34-44.
- [23] Falco G, Einicke GA., Malos JT, DAVIS F. 2012. Analysis of Constrained Loosely Coupled GNSS/INS Integration Solutions. *Sensors*. 12(11).
- [24] Cazzaniga N. E., Forlani G. and Roncella R. 2007. Improving the reliability of a GNSS/INS navigation solution for MM vehicles by photogrammetry. In 5-th International Symposium on Mobile Mapping Technology, Padova.
- [25] Scherzinger B. M. 2000. Precise robust positioning with inertial/GNSS RTK. In Proceedings of the 13th International Technical Meeting for the Satellite Division of the Institute of Navigation (ION GNSS) (pp. 115-162).
- [26] Artes F. and Hutton J. 2005. GNSS and Inertial Navigation Delivering. *GEOconnexion International Magazine*. pp. 52-53.
- [27] Habib A., Bang K. I., Kersting A. P. & Chow J. 2010. Alternative methodologies for LIDAR system calibration. *Remote Sensing*. 2(3): 874-907.
- [28] Zhang K., Chen S. C., Whitman D., Shyu M. L., Yan J. & Zhang C. 2003. A progressive morphological filter for removing nonground measurements from airborne LIDAR data. *IEEE transactions on geoscience and remote sensing*. 41(4): 872-882.
- [29] Morin K. and El-Sheimy N. 2002. Post-mission adjustment methods of airborne laser scanning data. In FIG XXII International Congress, Washington, DC USA.
- [30] Grünthal E., Gruno A. and Ellmann A. 2014. Monitoring of coastal processes by using airborne laser scanning data. In: *Environmental Engineering. Proceedings of the International Conference on Environmental Engineering. ICEE* (Vol. 9, p. 1). Vilnius Gediminas Technical University, Department of Construction Economics & Property.
- [31] Reporting, Horizontal Accuracy. 2007. ASPRS LIDAR Guidelines.
- [32] Vaughn C., Bufton J., Krabill W. and Rabine D. 1996. Georeferencing of airborne laser altimeter measurements. *International Journal of Remote Sensing*. 17(11): 2185-2200.
- [33] Barzaghi R., Carrion D., Pepe M. and Prezioso G. 2016. Computing the Deflection of the Vertical for Improving Aerial Surveys: A Comparison between EGM2008 and ITALGEO05 Estimates. *Sensors*. 16(8): 1168.
- [34] Board of Cultural Heritage of Pompeii, 2015, A Guide to the Pompeii Excavations. p. 34. Last accessed (April 19, 2017). <http://pompeiiisites.org/allegati/A%20Guide%20to%20the%20Pompeii%20Excavations.pdf>.
- [35] Welch K. 1994. The Roman arena in late-Republican Italy: A new interpretation. *Journal of Roman Archaeology*. 59-80. doi:10.1017/S1047759400012502.
- [36] Leica Geosystems ALS 500 II 2017. Airborne Laser Scanner Product Specifications. Last accessed. March 30, 2017. <http://www.nts-info.com/inventory/images/ALS50-II.Ref.703.pdf>.
- [37] Roth R. B. & Thompson J. 2008. Practical application of multiple pulse in air (MPIA) LIDAR in large-area surveys. *Proceedings of international archives of the photogrammetry, remote sensing and spatial information sciences*; pp.183-188.
- [38] Farr T. G., Rosen P. A., Caro E., Crippen R., Duren R., Hensley S. ... & Seal D. 2007. The shuttle radar topography mission. *Reviews of geophysics*. 45(2).



- [39] Selvan M. T., Ahmad S. A. R. F. A. R. A. Z. & Rashid S. M. 2011. Analysis of the geomorphometric parameters in high altitude glacierised terrain using SRTM DEM data in Central Himalaya, India. ARPJN Journal of Science and Technology. 1(1): 22-27.
- [40] Isenburg M. 2013. Laszip. Photogrammetric Engineering & Remote Sensing. 79(2): 209-217.
- [41] Pepe M., Prezioso G. 2015. A Matlab geodetic software for processing airborne LIDAR bathymetry data, ISPRS - International Archives of the Photogrammetry, Remote Sensing and Spatial Information Sciences. XL-5/W5: 167-170.